# Geomorphology and Climate Interact to Control Organic Carbon Stock and Age in Mountain River Valley Bottoms

**Daniel N. Scott[1*], Ellen Wohl[1]**

[1] Colorado State University, Department of Geosciences, Fort Collins, CO

Corresponding author: Daniel Scott (scott93@uw.edu)

* Current Affiliation: University of Washington, Department of Earth and Space Sciences, Seattle, WA

---



---

## Abstract

Organic carbon (OC) in valley bottom downed wood and soil that cycles over short to moderate timescales ($10^1$ to $10^5$ yr) represents a large, dynamic, and poorly quantified pool of carbon whose distribution and residence time affects global climate. We compare four disparate mountain river basins to show that mountain river valley bottoms store substantial estimated OC stocks in floodplain soil and downed wood ($127.3^{+24.5}_{-37.4}$ MgC/ha, n = 178). Although soil OC is generally young (exhibiting a median radiocarbon fraction modern value of $0.97^{+0.02}_{-0.01}$, n = 121), geomorphic processes regulate soil burial and processes that limit microbial respiration, preserving aged OC in certain parts of the river network. Statistical modeling of OC stocks suggests that biogeomorphic processes and the legacy of past erosion regulate the modern distribution of OC in river networks. Our results suggest that although mountain rivers may accumulate large OC stocks relatively rapidly, those stocks are highly sensitive to alterations in soil and wood retention, implying both short- and long-term feedbacks between retentiveness and the distribution of OC between the land and atmosphere.

## Plain Language Summary

Carbon stored on the land has the potential to be released to the atmosphere and act as a greenhouse gas, influencing global climate. To predict future climate, it is imperative to understand where and how much carbon is stored across the landscape to understand how much carbon might be released to and/or sequestered from the atmosphere in the future. We quantify carbon storage in downed wood and soil in mountain river valley bottoms, finding that mountain river valley bottoms are high magnitude carbon storage zones on the landscape, and that the legacy of past glaciation, climate, and modern erosional and depositional processes regulate the age and quantity of stored OC. Our results imply that human actions can change how much carbon is stored in mountain river valley bottoms, and how it is stored there. Understanding the distribution of carbon across the landscape, especially in carbon-rich zones such as valley bottoms, requires an understanding of both the historic and modern processes shaping the landscape and vegetation.

## 1 Introduction

Organic carbon (OC) stored in soil and organic material in freshwater systems is substantial (Aufdenkampe et al., 2011) and varies in both spatial distribution of concentration (Battin et al., 2008; Scott & Wohl, 2018b; Sutfin et al., 2016; Sutfin & Wohl, 2017; Wohl, Hall, et al., 2017) and residence time (Barnes et al., 2018; Marwick et al., 2015; Omengo et al., 2016). Carbon dynamics in these systems over short to moderate timescales ($10^1$ to $10^5$ yr) can thus strongly regulate carbon emissions to and sequestration from the atmosphere (Berner, 1990; Stallard, 1998), regulating global climate. Although numerous measurements have been made of the radiocarbon age of particulate OC in transport, especially in large river basins (e.g., Barnes et al., 2018; Schefuß et al., 2016; Tao et al., 2015; Xue et al., 2017), the stock and corresponding age (as indicated by radiocarbon activity) of OC stored in river corridors (*sensu* Harvey & Gooseff, 2015) have yet to be quantified in floodplains across individual basins. At the basin scale, OC export versus retention in freshwater systems is broadly controlled by sediment transport dynamics (Leithold et al., 2016), whereby increased sediment retention in floodplains may lead to the storage of OC over long timescales (Steger et al., 2019). We quantify OC stock and radiocarbon activity in floodplain soil at the reach to watershed scale across multiple disparate river basins to better understand how variability in hydrogeomorphic processes over short and long timescales influence riverine carbon storage across mountain river watersheds.

OC that enters the fluvial network can either be stored, commonly as downed wood or soil (Sutfin et al., 2016), or exported. Erosion regulates the fate of OC (Doetterl et al., 2016; Hilton, 2017; Wang et al., 2017) and whether that OC is stored long-term in sedimentary sinks (Blair & Aller, 2012) or respired to the atmosphere by microbes (Falloon et al., 2011; Jobbágy & Jackson, 2000). Modeling indicates that sedimentation dynamics should regulate the age of OC in floodplain soils (Torres et al., 2017), complementary to the idea that geomorphic processes regulate OC concentrations in those soils (Lininger et al., 2018; Scott & Wohl, 2018b; Sutfin & Wohl, 2017; Swinnen et al., 2019; Wohl, Hall, et al., 2017) and wood loads in valley bottoms (Scott & Wohl, 2018b).

Despite the importance of erosion and the transport of wood and soil in determining the fate of OC in river networks, there is still a need for extensive quantification of the valley bottom OC stock and its age. Here, we quantify the OC stock in downed wood and floodplain soil in four mountain river basins across the western United States. We also quantify the age of this OC stock with an expansive sample of radiocarbon activity of floodplain soil bulk carbon. In doing so, we present a novel characterization of an important component of the terrestrial carbon pool and determine the role of mountain river basins in terrestrial carbon dynamics. We contextualize this characterization in terms of the geomorphic and geologic history of the study basins to draw broad, testable inferences regarding the interactions between climate, geomorphology, and OC dynamics in valley bottoms.

## 2 Methods

This study was conducted alongside work presented in Scott & Wohl (2018a, 2018b), and hence shares many of the same methods with those two works.

### *2.1 Field Sites*

We quantified the valley bottom OC stock in wood and soil across the entirety of the river network in four disparate watersheds (Figure 1). The Middle Fork Snoqualmie, in the central Cascade Range of Washington, has a mean annual precipitation of 3.04 m (Oregon State University, 2004), 2079 m of relief, a 407 km$^2$ drainage area, and erosion rates ranging from 0.05 to 0.33 mm/yr (Reiners et al., 2003). The MF Snoqualmie exhibits glaciogenic topography with small glaciers still evident in headwaters and thick forests of fir and hemlock, with thinner, younger forests lower in the basin where clearcut logging was widespread over the last century. The MF Snoqualmie is dominated by tonalite, granodiorite, granite, and metamorphosed volcanic lithologies (dacite, andesite, and rhyolite), with sparse outcrops of rocks of the western mélange belt, including argillite, graywacke, and a single, ~0.03 km$^2$ outcrop of marble in the basin headwaters (Tabor et al., 1993). These sparse outcrops of potentially carbonate or petrogenic OC-bearing lithologies may introduce petrogenic OC to the river network, potentially complicating our use of LOI to obtain OC content and our interpretation of OC age (if radiocarbon-dead petrogenic carbon is present).

The Big Sandy, in the Wind River Range of Wyoming, exhibits a mean annual precipitation of 0.72 m (Oregon State University, 2004), 1630 m of relief, a 114 km$^2$ drainage area, and erosion rates that are likely significantly lower than those in basins studied in Washington, based on erosion rates < 0.1 mm/yr in nearby ranges (Garber, 2013; Kirchner et al., 2001). Similar to the MF Snoqualmie, the Big Sandy exhibits broad, glacially carved valleys and recently extensive glaciers (with remnants near summits), but generally sparse, parkland forests

(Fall, 1994) of pine, spruce, and fir with broad grassy meadows. Bedrock in the Big Sandy is entirely underlain by granitic and gneissic rocks (Sutherland & Scott, 2009), which we assume to bear no petrogenic OC or carbonates

The Sitkum and South Fork Calawah basins, in the Olympic Mountains of Washington, exhibit similar precipitation (3.61 and 3.67 m, respectively; Oregon State University, 2004), drainage area (112 and 85 $km^2$, respectively), identical 1024 m relief, and exhumation rates between 0.3 and 0.7 mm/yr (Brandon et al., 1998). Both basins exhibit deeply incised fluvial canyons, likely due to a lack of glacial erosion. Despite their similarity, the Sitkum has been extensively clearcut since the 1940s, whereas the SF Calawah is relatively pristine, residing in Olympic National Park (designated in 1938). Both basins are underlain by marine sedimentary rocks (Gerstel & Lingley Jr., 2000).

To simplify our presentation of results, we categorize these basins by climate and geomorphic legacy with respect to whether the valley bottoms display dominantly glaciogenic or fluviogenic topography. We term the MF Snoqualmie, with its moderate erosion rate, wet climate, and glaciogenic lakes and broad valley bottoms as the *wet glaciogenic* basin. In contrast, we term the Big Sandy, with its low erosion rate, semi-arid climate, and glaciogenic broad valley bottoms as the *semi-arid glaciogenic* basin. Finally, we term the Sitkum and SF Calawah, which exhibit the highest erosion rate, wettest climate, but most fluvially incised, narrow valley bottoms as the *wet fluviogenic* basins. We further subset the Sitkum as the *logged* wet fluviogenic basin and the SF Calawah as the *unlogged* wet fluviogenic basin.

*2.2 Site Selection and Sampling Strategy*

We stratified and randomly sampled soil and valley bottom characteristics in summer 2016 (both fluviogenic basins and the semi-arid glaciogenic basin) and summer 2017 (wet glaciogenic basin). For the purposes of sampling, we defined the valley bottom as the relatively lower slope portion of the landscape below hillsides that is likely shaped by fluvial processes, and exhibits a valley gradient less than 0.30 m/m, as measured on a 10 m DEM. In the wet fluviogenic basins, we randomly located five samples along each of five stream order strata in each basin. Due to accessibility issues, we surveyed 34 of the original 50 randomly sampled locations, which we supplemented with 16 subjectively chosen sites, for a total of 50 measured reaches. In the semi-arid glaciogenic basin, we were able to utilize a 10 m DEM and high-resolution aerial imagery to stratify the river network by confinement (unconfined if the channel width occupied less than half the valley bottom and confined otherwise) and then into five drainage area strata. We then randomly sampled five reaches in each of the ten resultant strata. Our eventual sample included 48 out of 50 randomly sampled sites, supplemented by 4 subjectively chosen sites, for a total of 52 samples. In the wet glaciogenic basin, we stratified the stream network by bed slope (from a 10 m DEM) into four strata, within which we randomly located ten sample sites. The large width of the floodplain in the lower portion of this basin necessitated separate stratification of that floodplain into individual geomorphic units (fill, point bar, oxbow lake, wetland, and undifferentiated floodplain). Within each of these units, we randomly sampled six points to take soil cores to supplement our soil sampling throughout the rest of the basin. This resulted in a total of 30 randomly sampled sites within the wet glaciogenic basin stratified by floodplain type in addition to 38 randomly sampled and eight subjectively sampled sites stratified by slope throughout the basin. Due to our sampling methodology, we distinguish sites in the wet glaciogenic basin by those stratified by slope (covering the entire basin) and those stratified by floodplain type (covering only the largest floodplains).

*2.3 Measuring Soil and Wood OC Stocks*

At each sample site in all four basins, we measured the total channel and floodplain wood load in jams and individual pieces within a reach surrounding the site defined as either 100 m or 10 channel widths, whichever was shorter (see Scott & Wohl (2018b) for detailed wood load measurement methodology). We converted total wood volume per unit area to wood OC mass per unit area (stock) by assuming a density based on estimated decay classes assigned to wood pieces and jams in the field (Harmon et al., 2011) and the approximation that half of the wood mass is carbon (Lamlom & Savidge, 2003). If soil was present, we also took a single soil core at a location on the floodplain of each site judged to be representative of the floodplain as a whole. We did not observe floodplain soils in the fluviogenic basins that were sufficiently fine textured to core (i.e., floodplains were limited in extent and dominantly comprised of coarse sand, gravel, cobble, and boulder material that likely has minimal organic matter), and as such, we consider those basins to store negligible soil OC. Wet glaciogenic basin sites stratified by floodplain type were not explicitly associated with a reach, so we did not measure wood load at those sites.

At all sites where floodplain soil was present, we collected cores to refusal or approximately 1 m depth (limited by our ability to carry coring equipment and soil to and from oftentimes remote field sites). Five of the 52 cores in the semi-arid glaciogenic basin, 12 of 46 cores in the wet glaciogenic basin sites stratified by slope, and 11 of 30 cores in the wet glaciogenic basin sites stratified by floodplain type did not reach refusal, indicating that while our estimates apply to the first meter of the soil profile, we likely underestimate the total soil OC stock in floodplain soils, especially in the wet glaciogenic basin. Soil samples were refrigerated within 1 - 48 hours after collection, then frozen until analysis.

To measure OC stock in soil, we used loss-on-ignition (LOI) of bulk soil samples (including coarse organic matter, such as buried wood pieces) after drying at 105 °C (to determine moisture) to estimate organic matter concentration, which we converted to OC concentration using a clay-held water correction (Hoogsteen et al., 2015) based on soil texture estimated by feel (Thien, 1979). We used a pedotransfer function (Adams, 1973) to estimate soil bulk density from organic matter (De Vos et al., 2005), allowing us to calculate soil OC stock at each site as the average OC concentration multiplied by bulk density, weighted by the proportion of the total core depth occupied by each sample. See (Scott & Wohl, 2018b) regarding the magnitude of the clay correction, estimates of carbonate concentrations in soils draining potentially carbonate-bearing rocks, and estimates of LOI accuracy compared to OC determined by CHN furnace. To summarize those methodological checks, carbonates are likely minimal in the samples we collected, and LOI is likely an unbiased estimate of OC concentration (Scott & Wohl, 2018b). The root mean square prediction error for this pedotransfer function is 0.24 g/cm$^3$, which represents a proportional uncertainty of 14.7% to 68.6% in our bulk density estimates, which range from approximately 0.35 to 1.63 g/cm$^3$. We discuss the potential implications of this uncertainty in the results.

Within each soil core, we tested for buried, high-OC concentration layers at depth due to the potential for such layers to be unusually aged or strongly influence OC stock at each site. We compared each buried soil sample to the sample above it using the criterion that a peak in OC at depth should have an OC concentration 1.5 times that of the overlying sample and be above 0.5 % by weight (Appling et al., 2014). More detailed analysis of these OC peaks is presented in Scott and Wohl (2018b)

*2.4 Field Measurements of Potential Controls on OC Stock, Soil Depth, and Fraction Modern*

Additional field measurements (listed in Table S1) were inconsistent across basins because field protocol evolved during the course of the study. We measured confinement and channel bed slope in all basins. We estimated a proxy for stream power by multiplying the drainage area, bed slope, and average basin-wide annual precipitation (from PRISM data; Oregon State University, 2004) at each reach. We also measured bankfull width and depth in the wet glaciogenic basin, bankfull width in the fluviogenic basins (generally equivalent to valley bottom width, because almost all reaches were tightly confined by their valley walls), and valley bottom width in the semi-arid glaciogenic basin. In the wet glaciogenic basin, we classified dominant bedform (Montgomery & Buffington, 1997), and classified streams as being either multithread or single thread. We also visually classified the dominant channel bed material as either sand (< 2mm), pebble (2-64 mm), cobble (64-256 mm), boulder (> 256 mm), or bedrock. We did not measure channel-specific variables for floodplain-stratified sites in the wet glaciogenic basin, because such sites were not clearly associated with a specific reach. We used a 10 m DEM and National Land Cover Database data (Homer et al., 2015) to measure elevation, the mean slope of the basin draining to each reach (including hillslopes and channels), canopy cover, land cover classification, and drainage area.

*2.5 Radiocarbon Analyses*

We randomly sampled across individual soil samples in the glaciogenic basins (the only two with floodplain soil) to select samples to be analyzed for $^{14}C$ activity. We randomly selected 11 soil samples in each of the four wet glaciogenic basin slope strata that had soil samples (the highest gradient stratum had so few samples that exhibited floodplain soil that we excluded it). We randomly selected 4 samples from each of the 5 wet glaciogenic basin floodplain type strata as well. In the semi-arid glaciogenic basin, we randomly selected six samples from each of the unique combinations of drainage area class and confinement strata. If too little soil was left after loss-on-ignition (LOI) analysis, we replaced the random sample with one of similar characteristics, if possible. This resulted in a total of 121 samples split between the glaciogenic basins that we analyzed for radiocarbon age.

We dried each radiocarbon sample in an oven at 100 °C for 24 hours before sending samples to DirectAMS (Zoppi et al., 2007) for radiocarbon analysis of bulk sediment, integrating all carbonaceous sediment sources other than macrobotanicals in the sample and providing an estimate of the distribution of radiocarbon activity of all soil OC that would be measured in a process such as LOI. We report radiocarbon ages as a fraction of modern (post 1950) radiocarbon, and at times, provide uncalibrated radiocarbon ages (based on the Libby half-life of 5,570 years) to contextualize fraction modern values.

Petrogenic OC can have a substantial effect on the radiocarbon activity of soils. To determine if petrogenic carbon may be present in soil samples, we fit a binary mixing model (i.e., a linear regression of OC concentration multiplied by radiocarbon fraction modern against OC concentration) (Galy et al., 2008) to estimate the proportion of petrogenic OC in soils that drained rocks that could potentially contain petrogenic OC (see Hilton, 2017, section 2.3 for a detailed explanation of this method). This method assumes that the floodplain sediment we sampled is well mixed, and that petrogenic carbon is derived from rocks approximately older than ~50 ka (the youngest metasedimentary rocks in this basin are mid-Cretaceous). The binary mixing model fit the data well ($R^2 = 0.99$, $p < 0.0001$). From this analysis, we found that the soil samples draining potentially petrogenic OC-bearing rocks in the wet glaciogenic basin (32 out of the 64 radiocarbon samples measured in that basin) likely contain negligible petrogenic OC (estimated at $-0.105^{+\,0.144}_{-\,0.155}$ % by weight based on 95% confidence interval of binary mixing model intercept and slope).

*2.6 Statistical Modeling and Comparisons*

We statistically modeled controls on OC stock, the radiocarbon fraction modern of floodplain soil OC, and soil depth (a proxy for valley bottom soil retention) using the R statistical package (R Core Team, 2017). Using multiple linear regression, we modeled the OC stock, soil depth, and median radiocarbon age in the glaciogenic basins, with individual sample sites (reaches) used as sample units for models of OC stock and soil depth, and individual soil samples used as sample units for modeling radiocarbon age. We separated the wet glaciogenic basin into slope and floodplain stratified sites for modeling due to differences in measured variables for each of those strata.

Our statistical modeling approach focused on testing relationships between hypothesized predictor variables (i.e., controls on OC stock, fraction modern, and soil depth) and the three aforementioned response variables of interest. We first performed univariate analysis between each hypothesized predictor and response, filtering out variables that appear to have a completely random relationship with the response based on visual examination, Wilcoxon rank-sum tests (Wilcoxon, 1945), and/or Spearman correlation coefficients. We then modeled each response variable using all subsets multiple linear regression with a corrected Akaike Information Criterion as a model selection criteria (Wagenmakers & Farrell, 2004). We iteratively transformed response variables to ensure homoscedasticity of error terms. To determine variable importance, we also considered sample size, effect magnitudes (β; the change in the response for a unit change in the predictor), and confidence intervals on effect magnitudes.

In addition to multivariate modeling, we performed comparisons to evaluate differences between basins. To do so, we used Wilcoxon rank-sum tests (Wilcoxon, 1945) due to the generally skewed distributions of our data, with a Holm multiple-comparison correction (Holm, 1979) when appropriate. We present uncertainties in both multivariate modeling and comparisons using 95% confidence intervals (CI) on estimates.

We compared our measured OC stocks in the wet glaciogenic basin to upland OC stocks in downed wood and soil using data from Smithwick et al. (2002), who measured those OC pools for uplands in the Washington Cascades. To determine total OC mass in the wet glaciogenic basin, we first estimated stream length for the entire network by sampling strata. We used our maps of unconfined floodplain surfaces and estimates of valley width for each stratum to compute a total valley bottom area for each stratum and for the entire basin, in addition to the total surface area (uplands and valley bottoms) for the basin (Table S2). We computed the OC mass in each stratum by multiplying the OC stock in both wood and soil by the valley bottom area for that stratum as appropriate. The OC mass for uplands was computed by multiplying estimates of the soil and downed wood OC stock data of Smithwick et al., (2002) for the Washington Cascades by the total non-valley bottom area of the basin. Using these estimates, we were able to compute the proportion of OC mass stored in valley bottoms as well as the proportion of total basin area taken up by valley bottoms. We computed uncertainty in these estimates by redoing calculations with the low and high end of the 95% confidence intervals on the median estimates for OC stock and valley width. Results of these computations are detailed in Table S2.

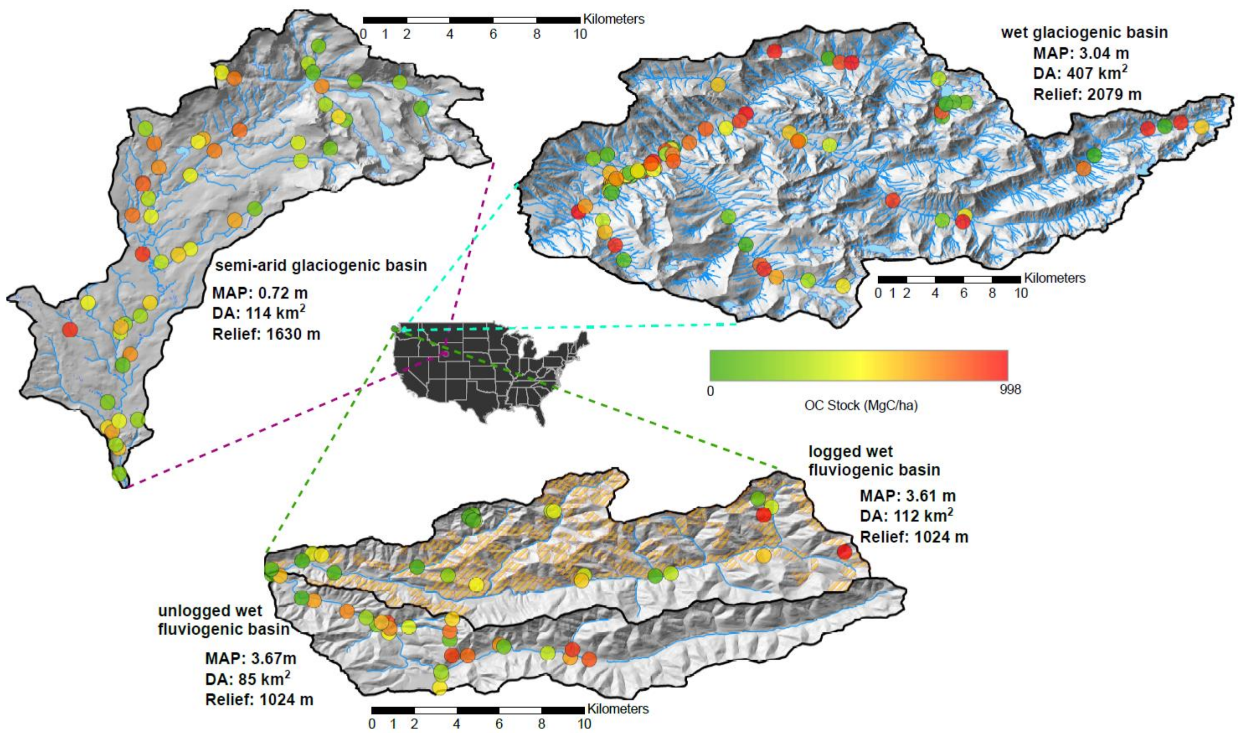


Figure 1. Map showing the location, topography, sampling sites, and stream network of the sampled basins, modified from Scott and Wohl (2018a). Clockwise, from upper left: Big Sandy (semi-arid glaciogenic) watershed, Wyoming; MF Snoqualmie (wet glaciogenic) watershed, Washington; Sitkum (logged wet fluviogenic, north) and SF Calawah (unlogged wet fluviogenic, south) watersheds, Washington. Circles represent sampling locations, colored by total OC stock (wood and soil). The orange overlay in the Sitkum basin represents areas that have experienced recorded clearcut timber harvest. Mean annual precipitation (MAP), drainage area (DA), and relief are given for each basin.

## 3 Results

### *3.1 Broad Trends in OC Storage and Distribution of OC Stocks between Soil and Wood*

Each basin stores different proportions of its total valley bottom carbon stock in soil versus downed wood (Figure 2, Table S3). Overall, we find that mountain river valley bottoms store substantial OC stocks in floodplain soil and downed wood ($127.3^{+24.5}_{-37.4}$ MgC/ha, n = 178), although this estimate does not account for uncertainty in our estimate of soil bulk density, only for variability among measured sites. Both wet, fluviogenic basins store only wood, with negligible soil. In the two glaciogenic basins that store OC in soil and wood, the percent of OC stored in soil is significantly different ($p < 0.0001$) between the semi-arid glaciogenic basin (n = 52, 95% CI on median between 95% and 100%) and wet glaciogenic basin sites stratified by slope (n = 44, 95% CI on median between 0% and 90%). Variability in wood load (linearly related to wood OC stock) in all three basins is discussed in detail in Scott & Wohl (2018b). Given the much greater proportion of OC stock in soil than in wood, we suggest that the uncertainties in OC soil stock associated with our use of a pedotransfer function do not change the overall interpretation of the relative importance of soil and wood OC stocks in the studied basins.

Valley bottoms may act as substantial OC pools, according to available data in the wet glaciogenic basin. Using estimates of valley bottom area and the total area of our wet, glaciogenic study basin, we find that valley bottoms take up only $5^{+7}_{-2}$ % ($2159^{+2795}_{-878}$ ha) of the total land surface area, but store $12^{+14}_{-9}$ % ($0.79^{+2.89}_{-0.69}$ Tg OC) of the total OC mass in the basin, indicating that valley bottoms, at least in this basin, are disproportionately important relative to the land area they occupy in storing OC. We note that the uncertainty in our estimate of total OC stock is substantial and compounded by the uncertainties of our soil OC concentration and soil bulk density estimation methods.

This is likely due to valley bottoms storing potentially more OC than comparable upland sites. Comparing wet glaciogenic basin sites (n = 74, 95% CI on median between 123.37 and 263.14 MgC/ha) to comparable upland sites (n = 10, 95% CI on median between 59.90 and 204.80 MgC/ha) measured by Smithwick et al. (2002), we find that valley bottom soil and downed wood may store higher OC stocks than are stored in coarse downed wood and soil in uplands, although we lack the precision to determine this robustly.

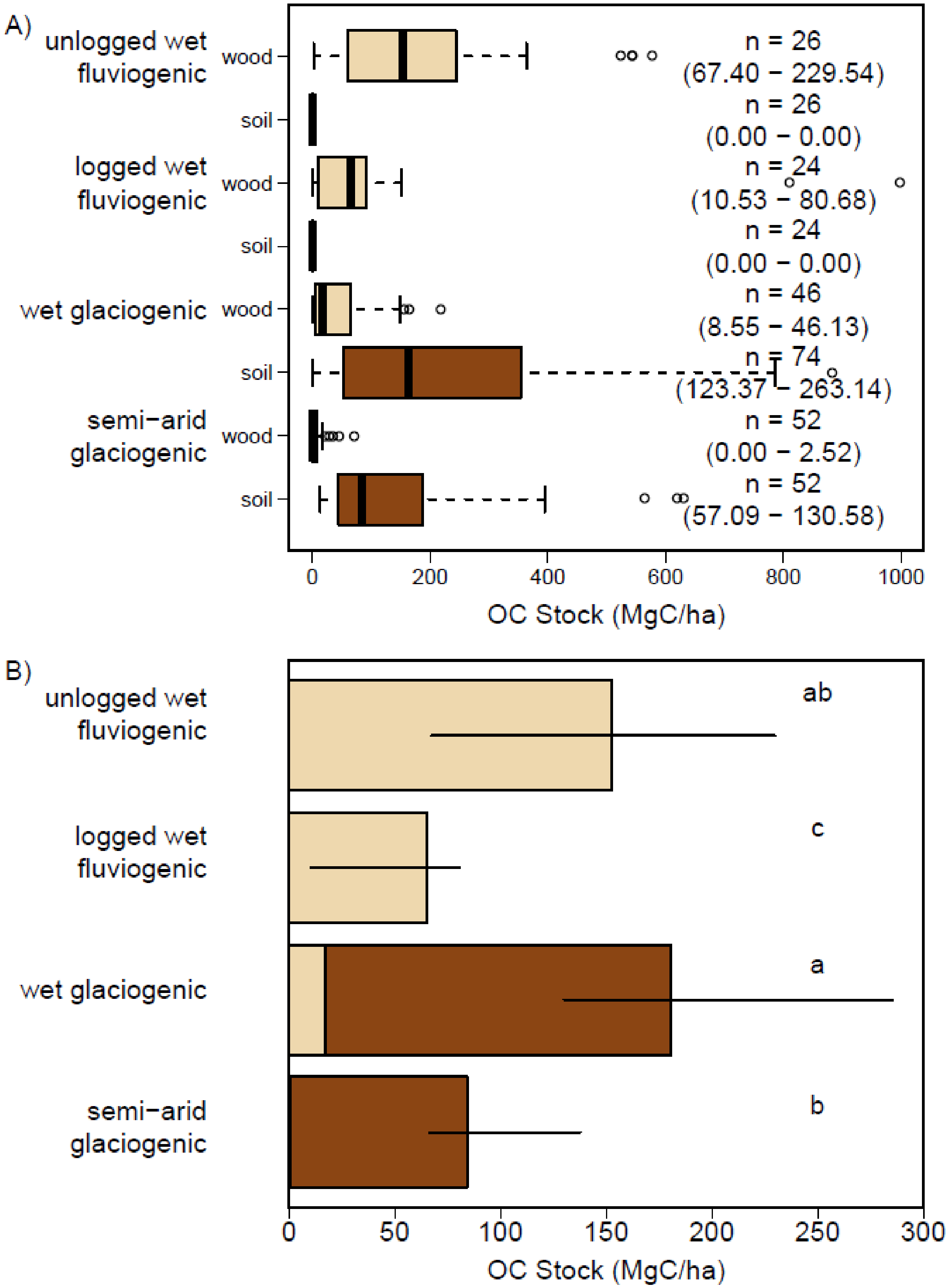
A)
unlogged wet fluviogenic
wood
soil
logged wet fluviogenic
wood
soil
wet glaciogenic
wood
soil
semi−arid glaciogenic
wood
soil
n = 26
(67.40 − 229.54)
n = 26
(0.00 − 0.00)
n = 24
(10.53 − 80.68)
n = 24
(0.00 − 0.00)
n = 46
(8.55 − 46.13)
n = 74
(123.37 − 263.14)
n = 52
(0.00 − 2.52)
n = 52
(57.09 − 130.58)
0
200
400
600
800
1000
OC Stock (MgC/ha)
B)
unlogged wet fluviogenic
logged wet fluviogenic
wet glaciogenic
semi−arid glaciogenic
ab
c
a
b
0
50
100
150
200
250
300
OC Stock (MgC/ha)

Figure 2. Boxplot of OC stock in wood (tan) and soil (brown) for each basin. Boxplots (A) show distribution of data, including the lack of soil in the SF Calawah and Sitkum (unlogged and logged wet fluviogenic basins, respectively). Bold lines represent median, box represents interquartile range, dashed lines represent 1.5 times the interquartile range, and circles represent outliers. Sample size (n) and 95% confidence interval on median estimates (shown in parentheses) are given for each group. Stacked bar plots (B) show the median total OC stock for each basin, separated into wood (tan) and soil (brown). Error bars represent the 95% CI on the median. Letters a-c represent groups with significant differences based on combined examination of 95% CI and pairwise Wilcoxon rank-sum tests. Note that the unlogged and logged wet fluviogenic basins contain negligible floodplain soil, and hence a zero value for soil OC stock.

### *3.2 Modeling Controls on OC Stock, Fraction Modern, and Soil Depth in Valley Bottoms*

Statistical modeling of OC stock, soil depth, and fraction modern in soil samples is summarized in Table 1. Table S4 details model selection. For each response variable, we present $\beta$ coefficient estimates for significant predictors that represent the change in the response for a unit change in the predictor.

Table 1. Summary of multiple linear regression models of OC stock, soil depth, and fraction modern. For each model group, response variable, sample size (n), proportion of the total variance explained by the model ($R^2$), and the equation describing model form are shown. Sample size (n) represents the number of individual sites (for OC stock and soil depth) or soil samples (for fraction modern) used to fit each model. For Model Form, response variables are abbreviated and shown with a transformation if a transformation was applied during modeling. In model equations, predictor variables are shown with units in brackets. For binary categorical variables (multithread, confinement, and standing water), brackets show the value corresponding to the coefficient shown. NA indicates that no significant model was found for the particular response variable.

| **Model Group** | **Response** | **n** | **$R^2$** | **Model Form** |
|---|---|---|---|---|
| Wet glaciogenic basin stratified by slope | OC (MgC/ha) | 44 | 0.88 | $OC^{\frac{1}{3}} = 0.70 + 0.069(Soil\ Depth\ [m]) + 0.014(Moisture\ [\%]) + 1.59(Multithread\ [present])$ |
| | Soil Depth (cm) | 44 | 0.56 | $SD^{\frac{1}{3}} = 1.69 - 4.79(Slope\ [m/m]) + 1.06(Confinement\ [unconfined])$ |
| | $^{14}C$ Fraction Modern | 44 | 0.54 | $FM = 1.06 - 0.0029(Soil\ Depth\ [m])$ |
| Wet glaciogenic basin stratified by floodplain type | OC (MgC/ha) | 30 | 0.67 | $OC = -61.10 + 3.35(Soil\ Depth\ [m]) + 1.17(Moisture\ [\%])$ |
| | Soil Depth (cm) | NA | NA | NA |
| | $^{14}C$ Fraction Modern | 20 | 0.32 | $FM = 1.07 - 0.0029(Soil\ Depth\ [m]) - 0.12(Standing\ Water\ [present])$ |
| Semi-arid glaciogenic basin | OC (MgC/ha) | 52 | 0.81 | $OC^{\frac{1}{3}} = 2.78 + 0.026(Soil\ Depth\ [m]) + 0.0093(Moisture\ [\%])$ |
| | Soil Depth (cm) | 52 | 0.47 | $SD^{\frac{1}{3}} = 5.73 - 1.68(Slope\ [m/m]) + 0.48(Confinement\ [unconfined]) - 0.00074(Elevation\ [m])$ |
| | $^{14}C$ Fraction Modern | 57 | 0.63 | $FM = 1.40 - 0.0028(Soil\ Depth\ [m]) - 0.00011(Elevation\ [m]) - 0.068(Confinement\ [unconfined])$ |

Soil moisture and depth dominantly control soil OC stock across both glaciogenic basins. In wet glaciogenic basin sites stratified by slope, soil OC stock is controlled by moisture content (β = 0.014 ± 0.0057), soil depth (β = 0.069 ± 0.011), and whether the reach is multithread (β = 1.59 ± 0.97). Soil OC stock in wet glaciogenic basin sites stratified by floodplain type is controlled by soil depth (β = 3.35 ± 1.15) and moisture (β = 1.17 ± 0.37). Soil OC stock in semi-arid glaciogenic basin sites is similarly controlled by soil depth (β = 0.026 ± 0.0066) and moisture (β = 0.0093 ± 0.0024).

Floodplain soil OC is dominantly modern in these study basins, despite exhibiting low fraction modern values (likely indicating preserved, aged OC) in certain environments (Figure 3). We found no significant difference in median radiocarbon age of floodplain OC between the two study basins. Bulk carbon in soils sampled in the semi-arid glaciogenic basin exhibit a median fraction modern of $0.98^{+0.02}_{-0.02}$, similar to the wet glaciogenic basin median fraction modern of $0.96^{+0.03}_{-0.03}$. Across both basins, the median fraction modern of sampled soils is $0.97^{+0.02}_{-0.01}$ (this corresponds to an uncalibrated radiocarbon age of approximately 245 yr BP). Despite the bulk of sampled soils being relatively young, both basins exhibited aged OC: In the semi-arid glaciogenic basin, 9 of the 57 (16%) samples tested exhibited fraction modern values less than 0.85 (corresponding to an uncalibrated radiocarbon age greater than approximately 1306 yr BP), compared to 10 of the 64 (16%) samples tested from the wet glaciogenic basin.

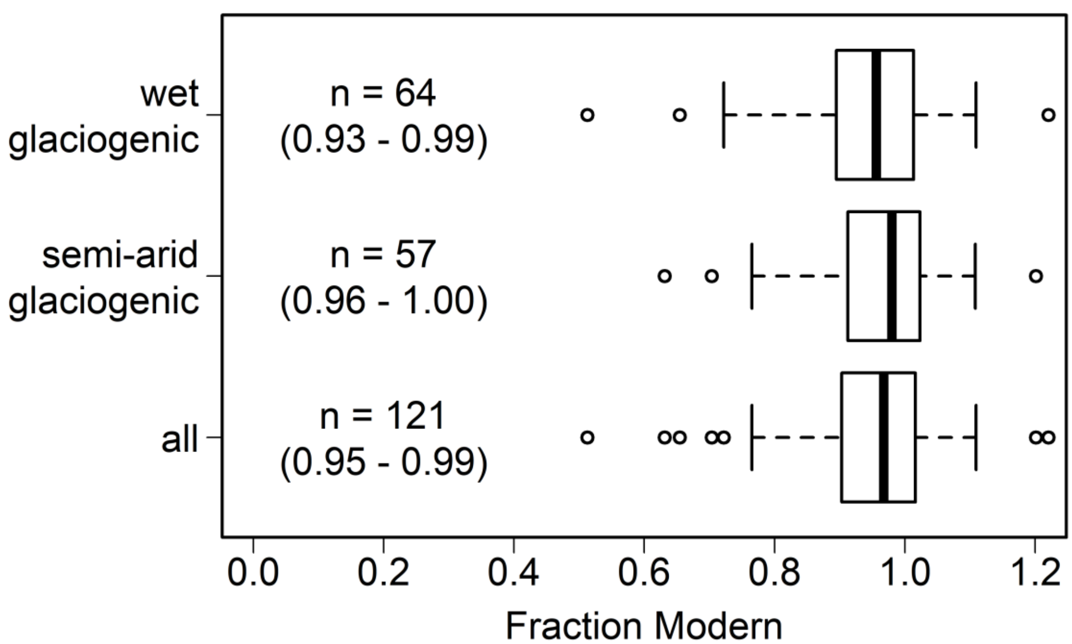


Figure 3. Boxplot of floodplain soil OC sample 14C fraction modern. Bold lines represent median, box represents interquartile range, dashed lines represent 1.5 times the interquartile range, and circles represent outliers. Sample size (n) and 95% confidence interval on median estimates (shown in parentheses) are given for each group. The median fraction modern of all sampled soils, $0.97^{+0.02}_{-0.01}$, corresponds to an uncalibrated radiocarbon age of approximately 245

yr BP, and the lowest measured fraction modern, 0.51, corresponds to an uncalibrated radiocarbon age of approximately 5370 yr BP.

These aged OC samples were generally found in deep soils (Figure 4), but also where streams are unconfined, at high elevations, and where standing water is present. In wet glaciogenic basin soil samples stratified by slope, fraction modern decreased (i.e., samples got older) with increasing sample depth below the ground surface ($\beta = -0.0029 \pm 0.00082$). In wet glaciogenic basin soil samples stratified by floodplain type, fraction modern decreased with sample depth below the ground surface ($\beta = -0.0029 \pm 0.0022$) and were lower when standing water was present at the sampled site ($\beta = -0.12 \pm 0.11$). In semi-arid glaciogenic basin soil samples, fraction modern decreased with increasing sample depth below ground surface ($\beta = -0.0028 \pm 0.00088$), with increasing elevation ($\beta = -0.00011 \pm 0.000074$), and where floodplains were unconfined ($\beta = -0.068 \pm 0.036$). Essentially, soil samples that resided in unconfined, deep, and high elevation sites (i.e., subalpine wetlands), tended to exhibit lower fraction modern values (i.e., were older). For example, the samples in the semi-arid basin that came from unconfined sites, sample depths greater than 25 cm below the ground surface, and elevations above 2750 m (12 of the 57 total samples from the basin) exhibited a median fraction modern value of $0.84^{+0.09}_{-0.08}$, which corresponds to an uncalibrated radiocarbon age of $1389^{+761}_{-818}$ yr BP.

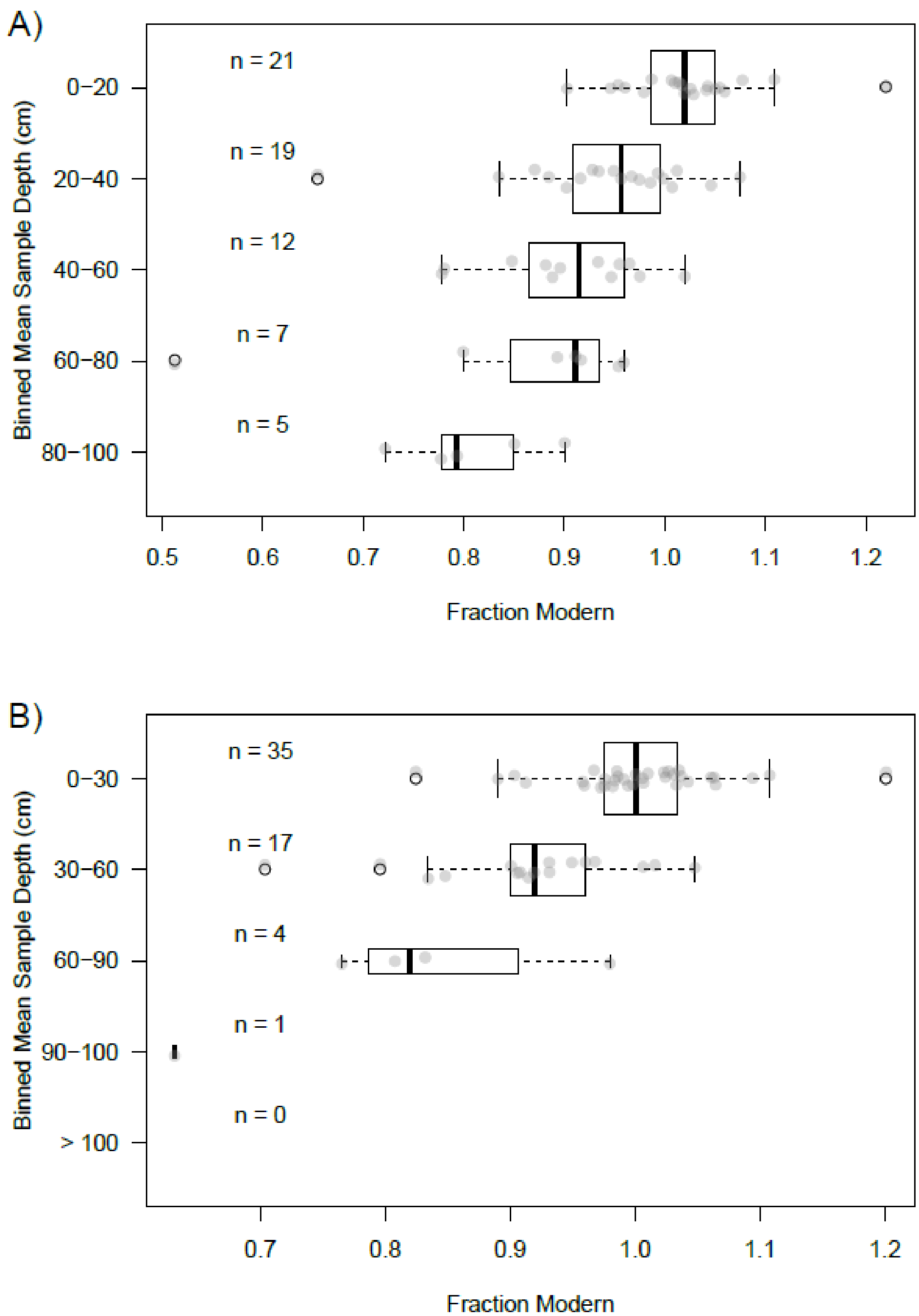


Figure 4. Boxplots of radiocarbon fraction modern binned by mean sample depth below the ground surface for the wet glaciogenic (A) and semi-arid glaciogenic (B) basins. Bold lines represent median, box represents interquartile range, dashed lines represent 1.5 times the interquartile range, and circles represent outliers. Transparent grey points show all data for each group. Sample size (n) is shown for each group.

Soil depth, a primary control on OC stock and fraction modern, is dominantly controlled by confinement and channel bed slope. Modeling soil depth as a proxy for soil retention in wet glaciogenic basin sites stratified by floodplain type yielded no significant results. Soil depth in wet glaciogenic basin sites stratified by slope is controlled by channel bed slope (β = -4.79 ±

2.14) and whether the stream is unconfined (β = 1.06 ± 0.64). Soil depth in semi-arid glaciogenic basin sites is controlled by elevation (β = -0.00074 ± 0.00080), channel bed slope (β = -1.68 ± 1.20), and whether the stream is unconfined (β = 0.48 ± 0.49). We note that while elevation and confinement in the semi-arid basin are not significant at a 95% confidence level, they are significant at a 90% confidence level, and we choose to interpret those effects as significant in regulating soil depth.

## 4 Discussion

*Increased soil retention (both in terms of valley width and soil depth) leads to the preservation of high magnitude OC stocks by storing deep soil over a larger area.* Our modeling results indicate that deeper soils tend to store higher OC stocks as well as more aged OC (Figure 4). OC is stored most effectively where buried sediment is less likely to be eroded (e.g., unconfined valleys with a presumably slower turnover rate in the semi-arid glaciogenic basin) (Cierjacks et al., 2011) and where microbial respiration is suppressed (e.g., where soil moisture is high or soils are saturated due to being near floodplain lakes in the wet glaciogenic basin). Where floodplains are sufficiently retentive, OC appears to be able to remain on the landscape for $10^2$ to $10^3$ yr timescales. Thus, along with likely storing more soil OC than uplands (Lininger et al., 2018; Wohl et al., 2012), floodplain soils appear capable of acting as effective transient pools of OC (e.g., Hoffmann et al., 2009). Burial of soil OC in wide, retentive valley bottoms is the dominant process in preserving old OC in these basins, a trend that fits with both modeling (Torres et al., 2017) and field observation (Barnes et al., 2018; Graf-Rosenfellner et al., 2016; Swinnen et al., 2019).

*Net changes in wood and soil retention due to activities such as forest harvest in the wet glaciogenic basin (Scott & Wohl, 2018a) have likely caused substantial redistribution of OC and potential sequestration lower in the network* (Wohl, Hall, et al., 2017; Wohl, Lininger, et al., 2017; Wohl & Scott, 2016). A century-scale turnover (assuming stocks are currently in steady state) of the majority of the substantial floodplain soil OC pool indicates that changes in soil retention and resulting storage of OC (e.g., due to land use change) should be tightly linked to OC respiration rate to the atmosphere over moderate timescales. Although OC likely turns over more rapidly in the mountainous basins studied here, it may be stored for longer periods of time lower in the river network after being eroded (Doetterl et al., 2016; Van Oost et al., 2012; Wang et al., 2017), depending on erosion and sedimentation dynamics (Schook et al., 2017; Torres et al., 2017). Changes in retention of the mountain river valley bottom OC stock may have rapid (due to generally short turnover times) and substantial (due to its high magnitude) effects on the distribution of OC between the atmosphere and terrestrial storage. Our modeling indicates that soil depth, a proxy for retention, is largely a function of erosivity (the efficiency of soil erosion and transport downstream), with wider, lower gradient valley bottoms storing deeper soils and more OC, and thus presenting a greater potential OC source if soil retention is decreased via disturbance. Wood load variability is likely a function of wood supply, governed by climate and land use, and spatial heterogeneity, which regulates how efficiently valley bottoms can trap wood (Scott & Wohl, 2018b).

*Our comparison of disparate basins shows that where there is an abundant source of wood (e.g., wet basins with dense forests), wood acts as a substantial OC pool (Scott & Wohl, 2018b). However, where forests are sparse (e.g., the semi-arid glaciogenic basin), soil is by far the dominant valley bottom OC pool.* When taken in the context of radiocarbon analyses of OC in larger rivers (Barnes et al., 2018; Schefuß et al., 2016; Xue et al., 2017), our results indicate substantially faster soil OC cycling in mountainous, headwater basins, in contrast to sites lower in river networks, where burial of OC may lead to longer OC preservation (Blazejewski et al., 2009; Ricker et al., 2013). However, deep soil burial in any portion of the network can lead to old OC ages (on the order of $10^3$ yr). Burial of wood in floodplains, which can lead to exceptionally long-term preservation, likely only occurs in wide, unconfined reaches.

The partitioning of OC between wood and soil has direct implications for best management practices in terms of restoring OC stocks to anthropogenically influenced valley bottoms. Wood retention is also likely easier and more commonly managed (Roni et al., 2015) than soil (Bullinger-Weber et al., 2014), as wood trapping structures or direct wood placement can both enhance wood loads. Our results imply that attempting to increase soil OC stock in wet, fluviogenic basins such as the Sitkum would likely be ineffective due to the naturally low soil retention in such a basin with deeply incised, narrow valleys. Restoring wood there, however, would likely increase the OC stock substantially, if the unlogged wet, fluviogenic basin in this study is representative of potential wood OC stocks. Still, a major uncertainty exists in terms of where wood is most stable on the landscape.

*Climate, by influencing forest characteristics and resulting litter input rates to soils and wood supply to channels, acts as a first-order control on the partitioning of OC between floodplain soil and wood as well as the total valley bottom OC stock.* In both the wet and semi-arid glaciogenic basins, floodplain soils store more OC stock than downed wood. However, if we take the unlogged wet fluviogenic basin as an example of wood loads in a pristine basin in the Pacific Northwest, it appears possible that wood OC stock can be of comparable magnitude to soil OC stock (in the wet glaciogenic basin). This implies a strong potential for increasing the OC stock in wood in the wet glaciogenic basin, in which wood loads are likely decreased as a result of logging (Scott & Wohl, 2018b). It is also important to note the significant difference between soil OC stocks in the wet versus semi-arid glaciogenic basin. Both of these basins have similar soil retention, as measured by median soil depth (Wilcoxon rank sum test $p = 0.85$, $n = 52$ for semi-arid glaciogenic basin and $n = 75$ for wet glaciogenic basin) and median valley bottom width (Wilcoxon rank sum test $p = 0.19$, $n = 52$ for semi-arid glaciogenic basin and $n = 75$ for wet glaciogenic basin), but OC concentrations in the wetter basin can be substantially higher than those in the semi-arid basin, potentially due to difference in OC inputs resulting from differing rates of litter input (Scott & Wohl, 2018b), which is likely a result of the difference in climate between the two basins.

*Comparing the distribution of OC between wood and soil in these basins reveals a strong impact of basin morphology, which is a result of uplift rate, erosion rate and style, and climate.* Where valley bottoms are narrow, likely due to a high precipitation rate and accompanying rates of fluvial incision, valleys store negligible amounts of soil, but forests grow dense and wood OC stock can be extremely high, as long as trees go unharvested and can be recruited to channels, as in the two study basins in the Olympics (Scott & Wohl, 2018a). In the semi-arid glaciogenic basin, low uplift rate, glaciogenic valleys, and dry climate correspond to broad valley bottoms but sparse forests, resulting in almost negligible wood OC stock (Scott & Wohl, 2018b) and only moderate soil OC storage, likely due primarily to low rates of litterfall input (Scott & Wohl, 2018b). Where the climate is wet, uplift is moderately high, but valleys are widened by recent glaciation, we observe both broad valley bottoms and dense forests, leading to substantial OC stocks in soil in the wet glaciogenic basin. Given that the wet glaciogenic basin has been extensively logged, it is likely that total OC stocks there were much higher than either the wet fluviogenic or semi-arid glaciogenic basins until the last century. Valley bottoms of the wet glaciogenic basin represent a peak in potential OC stock due to dense forests; wide, retentive valley bottoms; and high rates of OC input from vegetation.

## 5 Conclusion

The legacies of glaciation and tectonics, combined with geomorphic processes, determine the distribution, magnitude, and age of the transient OC stock in mountain river valley bottoms. Here, we show through extensive field measurement that this OC pool is highly variable both spatially and temporally, but that geomorphic processes largely explain that variation. Burial and preservation of OC-rich soil is essential to preserving soil OC for long periods of time. Deeper, wetter soils that likely have lower rates of microbial respiration exhibit radiocarbon ages up to $10^3$ yr. Such deep soils are found in unconfined valleys that show the legacy of both tectonics and past glaciation. Climate also plays a role by regulating OC inputs and respiration (Scott & Wohl, 2018b), in turn determining how much OC is available to be stored in a valley bottom of a given retentiveness.

Valley bottom geometry, forest stand characteristics (directly affected by land use), and climate interact to regulate the retention of both wood (Scott & Wohl, 2018b) and soil. This implies that managing the substantial valley bottom OC stock in soil and wood necessitates a careful consideration of geomorphic process and form. However, in general, our results support the idea that less morphologically dynamic portions of floodplain tend to accumulate substantial OC (Cierjacks et al., 2011; Sutfin & Wohl, 2017). Future examination of carbon sequestration efforts in river corridors (e.g., Bullinger-Weber et al., 2014) will test this inference by determining the rate and magnitude at which OC can be restored to floodplain soils in varying environments. We note that our estimates of OC stock are highly uncertain, based on both variability between samples as well as measurement uncertainty. Because management seeking to preserve or sequester OC in valley bottoms depends on an accurate accounting of OC stocks, and because of the difficulty of collecting these data, future work to more efficiently and accurately quantify OC stocks in soil and wood will likely have substantial benefits for management of landscape OC storage.

Anthropogenic and natural alterations to soil retention likely influence riverine OC storage and transport, with potential feedbacks between OC distribution, climate, and geomorphic processes that further regulate soil retention. The century-scale age of much of the soil OC measured in these basins implies a close coupling between soil retention and the distribution of OC across the landscape and between the land and atmosphere. The alteration of valley bottom morphology and soil retention likely influences the fate of OC sequestered in high primary productivity (Schimel & Braswell, 2005) mountain ranges over short (Wohl, Hall, et al., 2017; Wohl, Lininger, et al., 2017) and long (Berner, 1990; Molnar & England, 1990) timescales. Changes in soil retention likely alter how much OC reaches downstream water bodies that may sequester OC over longer timescales, thus altering the respiration of that OC to the atmosphere. The distribution of OC between the land and atmosphere regulates global climate, which can in turn regulate the hydrologic, biotic, and geomorphic processes that regulate soil retention, as we show here, as well as OC concentration (Scott & Wohl, 2018b). Future work to quantify the residence time and decay rate of wood in valley bottoms and its eventual fate when exported, in addition to examination of the sources and fate of soil OC, will further constrain this feedback and the timescales at which it is relevant.

Our results indicate that, although mountainous river networks tend to be considered transport-dominated portions of a river network, retentive segments of mountainous river valleys can store substantial quantities of non-modern OC. The details of these carbon stocks reflect the interactions of climate, which influences OC inputs, and tectonics, which influences basin morphology. Consequently, climate and tectonics interact to regulate the distribution and magnitude of valley bottom OC storage.

**Acknowledgements**

This work was funded by NSF grant EAR-1562713 and a National Geographic Society Young Explorer Grant. We thank the Quileute tribe and Olympic National Park for access to field sites in the Olympics. We thank Ellen Daugherty for assistance in field work, Sarah Lowe for assistance processing soil samples, and Katherine Lininger for discussion and review that improved the manuscript. Data can be found in Data Set S1 and the Colorado State University Digital Repository (https://hdl.handle.net/10217/187763).

## References


Adams, W. A. (1973). The Effect of Organic Matter on the Bulk and True Densities of Some Uncultivated Podzolic Soils. *Journal of Soil Science*, *24*(1), 10–17. https://doi.org/10.1111/j.1365-2389.1973.tb00737.x

Adams, W. A. (1973). The Effect of Organic Matter on the Bulk and True Densitites of Some Uncultivated Podzolic Soils. *Journal of Soil Science*, *24*(1), 10–17. https://doi.org/10.1111/j.1365-2389.1973.tb00737.x

Appling, A. P., Bernhardt, E. S., & Stanford, J. A. (2014). Floodplain biogeochemical mosaics: A multi-dimensional view of alluvial soils. *Journal of Geophysical Research: Biogeosciences*, *119*(8), 1538–1553. https://doi.org/10.1002/2013JG002543

Aufdenkampe, A. K., Mayorga, E., Raymond, P. A., Melack, J. M., Doney, S. C., Alin, S. R., et al. (2011). Riverine coupling of biogeochemical cycles between land, oceans, and atmosphere. *Frontiers in Ecology and the Environment*, *9*, 53–60. https://doi.org/10.1890/100014

Barnes, R. T., Butman, D. E., Wilson, H., & Raymond, P. A. (2018). Riverine export of aged carbon driven by flow path depth and residence time. *Environmental Science and Technology*. https://doi.org/10.1021/acs.est.7b04717

Battin, T. J., Kaplan, L. a., Findlay, S., Hopkinson, C. S., Marti, E., Packman, A. I., et al. (2008). Biophysical controls on organic carbon fluxes in fluvial networks. *Nature Geoscience*, *1*(8), 95–100. https://doi.org/10.1038/ngeo602

Berner, R. A. (1990). Global biogeochemical cycles of carbon and sulfur and atmospheric O2 over phanerozoic time. *Chemical Geology*, *84*(1–4), 159.

Blair, N. E., & Aller, R. C. (2012). The Fate of Terrestrial Organic Carbon in the Marine Environment. *Annual Review of Marine Science*, *4*(1), 401–423. https://doi.org/10.1146/annurev-marine-120709-142717

Blazejewski, G. A., Stolt, M. H., Gold, A. J., Gurwick, N., & Groffman, P. M. (2009). Spatial Distribution of Carbon in the Subsurface of Riparian Zones. *Soil Science Society of America Journal*, *73*(5), 1733. https://doi.org/10.2136/sssaj2007.0386

Brandon, K. A., Roden-Tice, T. M., & Garver, J. I. (1998). Late Cenozoic exhumation of the cascadia accretionnary wedge in the Olympic montains, northwest Washington State. *Geological Society of America Bulletin*, *110*(8), 985–1009. https://doi.org/10.1130/0016-7606(1998)110<0985:LCEOTC>2.3.CO;2

Bullinger-Weber, G., Le Bayon, R.-C. C., Thébault, A., Schlaepfer, R., & Guenat, C. (2014). Carbon storage and soil organic matter stabilisation in near-natural, restored and embanked Swiss floodplains. *Geoderma*, *228–229*, 122–131. https://doi.org/10.1016/j.geoderma.2013.12.029

Cierjacks, A., Kleinschmit, B., Kowarik, I., Graf, M., & Lang, F. (2011). Organic Matter Distribution in Floodplains Can Be Predicted Using Spatial and Vegetation Structure Data. *River Research and Applications*, *27*, 1048–1057. https://doi.org/10.1002/rra.1409

Doetterl, S., Berhe, A. A., Nadeu, E., Wang, Z., Sommer, M., & Fiener, P. (2016). Erosion, deposition and soil carbon: A review of process-level controls, experimental tools and models to address C cycling in dynamic landscapes. *Earth-Science Reviews, 154,* 102–122. https://doi.org/10.1016/j.earscirev.2015.12.005

Fall, P. L. (1994). Modern Pollen Spectra and Vegetation in the Wind River Range, Wyoming, U.S.A. *Arctic and Alpine Research*, *26*(4), 383–392.

Falloon, P., Jones, C. D., Ades, M., & Paul, K. (2011). Direct soil moisture controls of future global soil carbon changes: An important source of uncertainty. *Global Biogeochemical Cycles*, *25*(3), 1–14. https://doi.org/10.1029/2010GB003938

Galy, V., Beyssac, O., France-Lanord, C., & Eglinton, T. (2008). Geological Stabilization of Carbon in the Crust Recycling of Graphite During Stabilization of Carbon in the Crust. *Science*, *322*, 943–946. https://doi.org/10.1126/science.1161408

Garber, J. (2013). *Using in situ cosmogenic radionuclides to constrain millenial scale denudation rates and chemical weathering rates on the Colorado Front Range*. Colorado State University.

Gerstel, W. J., & Lingley Jr., W. S. (2000). *Geologic Map of the Forks 1:100,000 Quadrangle, Washington*.

Graf-Rosenfellner, M., Cierjacks, A., Kleinschmit, B., & Lang, F. (2016). Soil formation and its implications for stabilization of soil organic matter in the riparian zone. *Catena*, *139*, 9–18. https://doi.org/10.1016/j.catena.2015.11.010

Harmon, M. E., Woodall, C. W., & Sexton, J. (2011). *Standing and Downed Dead Tree Wood Density Reduction Factors : A Comparison Across Decay Classes and Tree Species*. *Research Paper NRS-15*.

Harvey, J. W., & Gooseff, M. (2015). River corridor science: Hydrologic exchange and ecological consequences frombedforms to basins. *Water Resources Research*, *51*, 6893–6922. https://doi.org/10.1002/ 2015WR017617

Hilton, R. G. (2017). Climate regulates the erosional carbon export from the terrestrial biosphere. *Geomorphology*, *277*, 118–132. https://doi.org/10.1016/j.geomorph.2016.03.028

Hoffmann, T., Glatzel, S., & Dikau, R. (2009). A carbon storage perspective on alluvial sediment storage in the Rhine catchment. *Geomorphology*, *108*(1–2), 127–137. https://doi.org/10.1016/j.geomorph.2007.11.015

Holm, S. (1979). A Simple Sequentially Rejective Multiple Test Procedure. *Scandinavian Journal of Statistics*, *6*(2), 65–70.

Homer, C. G., Dewitz, J. A., Yang, L., Jin, S., Danielson, P., Xian, G., et al. (2015). Completion of the 2011 National Land Cover Database for the conterminous United States-Representing a decade of land cover change information. *Photogrammetric Engineering and Remote Sensing*, *81*(5), 345–354.

Hoogsteen, M. J. J., Lantinga, E. A., Bakker, E. J., Groot, J. C. J., & Tittonell, P. A. (2015). Estimating soil organic carbon through loss on ignition: Effects of ignition conditions and structural water loss. *European Journal of Soil Science*, *66*(2), 320–328. https://doi.org/10.1111/ejss.12224

Jobbágy, E. G., & Jackson, R. B. (2000). The vertical distribution of soil organic carbon and its relation to climate and vegetation. *Ecological Applications*, *10*(2), 423–436. https://doi.org/10.1890/1051-0761(2000)010[0423:TVDOSO]2.0.CO;2

Kirchner, J. W., Finkel, R. C., Riebe, C. S., Granger, D. E., Clayton, J. L., King, J. G., et al. (2001). Mountain erosion over 10 yr , 10 k.y., and 10 m.y. time scales. *Geology*, *29*(7), 591–594.

Lamlom, S. H., & Savidge, R. A. (2003). A reassessment of carbon content in wood: Variation within and between 41 North American species. *Biomass and Bioenergy*, *25*(4), 381–388. https://doi.org/10.1016/S0961-9534(03)00033-3

Leithold, E. L., Blair, N. E., & Wegmann, K. W. (2016). Source-to-sink sedimentary systems and global carbon burial: A river runs through it. *Earth-Science Reviews*, *153*, 30–42.

https://doi.org/10.1016/j.earscirev.2015.10.011
Lininger, K. B. B., Wohl, E., & Rose, J. R. R. (2018). Geomorphic Controls on Floodplain Soil Organic Carbon in the Yukon Flats, Interior Alaska, From Reach to River Basin Scales. *Water Resources Research*, 1934–1951. https://doi.org/10.1002/2017WR022042
Marwick, T. R., Tamooh, F., Teodoru, C. R., Borges, A. V., Darchambeau, F., & Bouillon, S. (2015). The age of river-transported carbon: A global perspective. *Global Biogeochemical Cycles*, *29*, 122–137. https://doi.org/10.1002/2014GB004911.Received
Molnar, P., & England, P. (1990). Late Cenozoic uplift of mountain ranges and global climate change: chicken or egg? *Nature*, *346*(6279), 29–34. https://doi.org/10.1038/346029a0
Montgomery, D. R., & Buffington, J. M. (1997). Channel-reach morphology in mountain drainage basins. *Bulletin of the Geological Society of America*, *109*(5), 596–611.
Omengo, F. O., Geeraert, N., Bouillon, S., & Govers, G. (2016). Deposition and fate of organic carbon in floodplains along a tropical semiarid lowland river (Tana River, Kenya). *Journal of Geophysical Research G: Biogeosciences*, *121*(4), 1131–1143. https://doi.org/10.1002/2015JG003288
Van Oost, K., Verstraeten, G., Doetterl, S., Notebaert, B., Wiaux, F., Broothaerts, N., & Six, J. (2012). Legacy of human-induced C erosion and burial on soil-atmosphere C exchange. *Proceedings of the National Academy of Sciences of the United States of America*, *109*, 19492–19497. https://doi.org/10.1073/pnas.1211162109
Oregon State University. (2004). PRISM Climate Group.
R Core Team. (2019). R: A Language and Environment for Statistical Computing. Vienna, Austria: R Foundation for Statistical Computing.
Reiners, P. W., Ehlers, T. A., Mitchell, S. G., & Montgomery, D. R. (2003). Coupled spatial variations in precipitation and long-term erosion rates across the Washington Cascades. *Nature*, *426*(001), 645–647. https://doi.org/10.1038/nature02111
Ricker, M. C., Stolt, M. H., Donohue, S. W., Blazejewski, G. A., & Zavada, M. S. (2013). Soil Organic Carbon Pools in Riparian Landscapes of Southern New England. *Soil Science Society of America Journal*, *77*(3), 1070–1079. https://doi.org/10.2136/sssaj2012.0297
Roni, P., Beechie, T., Pess, G., Hanson, K., & Jonsson, B. (2015). Wood placement in river restoration: fact, fiction, and future direction. *Canadian Journal of Fisheries and Aquatic Sciences*, *72*(3), 466–478. https://doi.org/10.1139/cjfas-2014-0344
Schefuß, E., Eglinton, T. I., Spencer-Jones, C. L., Rullkötter, J., De Pol-Holz, R., Talbot, H. M., et al. (2016). Hydrologic control of carbon cycling and aged carbon discharge in the Congo River basin. *Nature Geoscience*, *9*(9), 687–690. https://doi.org/10.1038/ngeo2778
Schimel, D. S., & Braswell, B. H. (2005). The role of mid-latitude mountains in the carbon cycle: Global perspective and a Western U.S. case study. In U. M. Huber, H. K. M. Bugmann, & M. A. Reasoner (Eds.), *Global Change and Mountain Regions* (pp. 449–456). Springer.
Schook, D. M., Rathburn, S. L., Friedman, J. M., & Wolf, J. M. (2017). A 184-year record of river meander migration from tree rings, aerial imagery, and cross sections. *Geomorphology*, *293*(June), 227–239. https://doi.org/10.1016/j.geomorph.2017.06.001
Scott, D. N., & Wohl, E. (2018a). Natural and Anthropogenic Controls on Wood Loads in River Corridors of the Rocky, Cascade, and Olympic Mountains, USA. *Water Resources Research*. https://doi.org/https://hdl.handle.net/10217/186057
Scott, D. N., & Wohl, E. E. (2018b). Geomorphic regulation of floodplain soil organic carbon concentration in watersheds of the Rocky and Cascade Mountains, USA. *Earth Surface*

*Dynamics*, *6*, 1101–1114. https://doi.org/10.5194/esurf-6-1101-2018

Smithwick, E., Harmon, M. E., Remillard, S. M., Acker, S. A., & Franklin, J. F. (2002). Potential upper bounds of carbon stores in forests of the Pacific Northwest. *Ecological Applications*, *12*(5), 1303–1317. https://doi.org/10.1890/1051-0761(2002)012[1303:PUBOCS]2.0.CO;2

Stallard, R. F. (1998). Terrestrial sedimentation and the carbon cycle: Coupling weathering and erosion to carbon burial. *Global Biogeochemical Cycles*, *12*(2), 231–257. https://doi.org/10.1029/98GB00741

Steger, K., Fiener, P., Marvin-DiPasquale, M., Viers, J. H., & Smart, D. R. (2019). Human-induced and natural carbon storage in floodplains of the Central Valley of California. *Science of the Total Environment*, *651*, 851–858. https://doi.org/10.1016/j.scitotenv.2018.09.205

Sutfin, N. A., & Wohl, E. (2017). Substantial soil organic carbon retention along floodplains of mountain streams. *Journal of Geophysical Research: Earth Surface*, *122*(7), 1325–1338. https://doi.org/10.1002/2016JF004004

Sutfin, N. A., Wohl, E., & Dwire, K. A. (2016). Banking carbon: A review of organic carbon storage and physical factors influencing retention in floodplains and riparian ecosystems. *Earth Surface Processes and Landforms*, *60*, 38–60. https://doi.org/10.1002/esp.3857

Sutherland, W. M., & Scott, J. E. (2009). *Preliminary geologic map of the Pinedale Quadrangle*.

Swinnen, W., Daniëls, T., Maurer, E., Broothaerts, N., & Verstraeten, G. (2019). Geomorphic controls on floodplain sediment and soil organic carbon storage in a Scottish mountain river. *Earth Surface Processes and Landforms*, 0–1. https://doi.org/10.1002/esp.4729

Tabor, R. W., Frizzell Jr, V. A., Booth, D. B., Waitt, R. B., Whetten, J. T., & Zartman, R. E. (1993). *Geologic map of the Skykomish River 30-by 60-minute quadrangle, Washington*.

Tao, S., Eglinton, T. I., Montluçon, D. B., McIntyre, C., & Zhao, M. (2015). Pre-aged soil organic carbon as a major component of the Yellow River suspended load: Regional significance and global relevance. *Earth and Planetary Science Letters*, *414*, 77–86. https://doi.org/10.1016/j.epsl.2015.01.004

Thien, S. J. (1979). A flow diagram for teaching texture-by-feel analysis. *Journal of Agronomic Education*, *8*(2).

Torres, M. A., Limaye, A. B., Ganti, V., Lamb, M. P., Joshua West, A., & Fischer, W. W. (2017). Model predictions of long-lived storage of organic carbon in river deposits. *Earth Surface Dynamics*, *5*(4), 711–730. https://doi.org/10.5194/esurf-5-711-2017

De Vos, B., Van Meirvenne, M., Quataert, P., Deckers, J., & Muys, B. (2005). Predictive Quality of Pedotransfer Functions for Estimating Bulk Density of Forest Soils. *Soil Science Society of America Journal*, *69*(i), 500–510. https://doi.org/10.2136/sssaj2005.0500

Wagenmakers, E.-J., & Farrell, S. (2004). AIC model selection using Akaike weights. *Psychonomic Bulletin & Review*, *11*(1), 192–196. https://doi.org/10.3758/BF03206482

Wang, Z., Hoffmann, T., Six, J., Kaplan, J. O., Govers, G., Doetterl, S., & Van Oost, K. (2017). Human-induced erosion has offset one-third of carbon emissions from land cover change. *Nature Climate Change*, *7*(5), 345–349. https://doi.org/10.1038/nclimate3263

Wilcoxon, F. (1945). Individual Comparisons by Ranking Methods. *Biometrics Bulletin*, *1*(6), 80–83. https://doi.org/10.2307/3001946

Wohl, E., & Scott, D. N. (2016). Wood and sediment storage and dynamics in river corridors. *Earth Surface Processes and Landforms*, n/a-n/a. https://doi.org/10.1002/esp.3909

Wohl, E., Dwire, K., Sutfin, N., Polvi, L., & Bazan, R. (2012). Mechanisms of carbon storage in mountainous headwater rivers. *Nature Communications*, *3*, 1263.

https://doi.org/10.1038/ncomms2274
Wohl, E., Hall, R. O., Lininger, K. B., Sutfin, N. A., & Walters, D. M. (2017). Carbon dynamics of river corridors and the effects of human alterations. *Ecological Monographs*, *87*(3), 379–409. https://doi.org/10.1002/ecm.1261
Wohl, E., Lininger, K. B., & Scott, D. N. (2017). River beads as a conceptual framework for building carbon storage and resilience to extreme climate events into river management. *Biogeochemistry*. https://doi.org/10.1007/s10533-017-0397-7
Xue, Y., Zou, L., Ge, T., & Wang, X. (2017). Mobilization and export of millennial-aged organic carbon by the Yellow River. *Limnology and Oceanography*, *13*. https://doi.org/10.1002/lno.10579
Zoppi, U., Crye, J., & Song, Q. (2007). Performance evaluation of the new AMS system at Accium BioSciences. *Radiocarbon*, *49*(1), 171–180.